ACS APPLIED MATERIALS & INTERFACES

Research Article

www.acsami.org

Electro-optic Coefficient Enhancement of $Al_xGa_{1-x}N$ via Multiple Field Modulations

Wei Jiang,[†,‡] Yaping Wu,[†] Wei Lin,[*,†] Shuping Li,[†] and Junyong Kang[*,†]

[†]Fujian Provincial Key Laboratory of Semiconductor Materials and Applications, Department of Physics, Xiamen University, Xiamen 361005, P. R. China

[‡]Xiamen Changelight Company Limited, Xiamen 361101, P. R. China

ABSTRACT: AlGaN has attracted growing interest for applications in electro-optic devices that generate and process optical signals. To enhance the electric-optic effect with polarity, we designed and grew GaN/$Al_xGa_{1-x}N$ quantum structures with x of about 0.5 by metal−organic vapor-phase epitaxy. Spectroscopic ellipsometry measurement and ab initio calculation demonstrated that the stronger polarization fields induced by higher Al contents in the barrier result in larger electro-optic effects. By applying external biases directly on both sides of these quantum structures, a high intensity of external field was achieved, and extraordinary and ordinary refractive indices were characterized by fitting the variable-angle spectroscopic ellipsometry. The values of deduced electric-optic coefficients were significantly enhanced by combining the resonance effect with the internal and external fields. Given the comparable electric-optic coefficients with conventional electro-optic crystals, AlGaN is an attractive candidate for nonlinear optical material, which provides a basis for large-scale integrations of ultraviolet electro-optic devices based on nitride semiconductors.

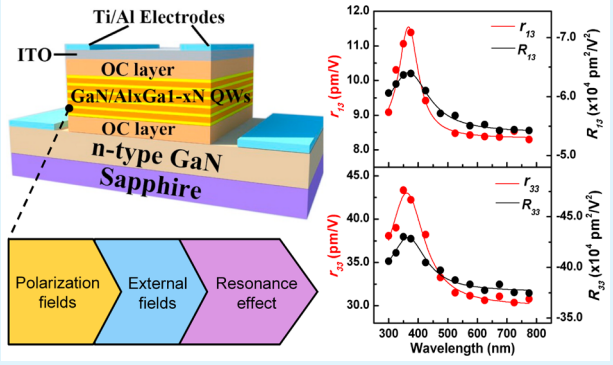

KEYWORDS: *AlGaN, electro-optic material, UV, quantum structure, III−V semiconductors*

INTRODUCTION

Electro-optic (EO) materials with second-order nonlinearity, such as KH_2PO_4 (KDP) and $LiNbO_3$ (LN), are new devices fundamental for nonlinear frequency conversion, electro-optic modulation, optical switch, and other optical elements in scientific and technical areas.[1−4] Driven by the desire for shorter wavelength response, the design and fabrication of such devices have motivated great interest in developing nonlinear optical materials with a large optical response.[5] Crystallographic noncentrosymmetry is a necessary feature in the structure of second order nonlinear optical crystals.[6] After the commercialization of GaN-based blue LEDs in the 1990s, GaN with an acentric structure, wurzite crystal, has been believed to be a promising material for next-generation optoelectronic devices operating in the ultraviolet (UV) region.[7−9] Devices performing both optical and electrical operations in the short wavelength region on a single low-cost chip are also aimed to be integrated.[10] The constituent materials are not compatible with other materials and devices within the same chip. Nevertheless, the EO coefficients of GaN-based materials are less than ideal for producing a significant EO effect compared with other traditional materials. Thus, extensive efforts have been made to amplify nonlinear optical responses. Previous reports revealed that EO coefficients can be effectively enhanced by applying an external electric field.[11,12] The internal polarization field of noncentrosymmetric polar crystals turns to be an extra degree of freedom for controlling the EO effect in addition to the external electric field. In this respect, recent investigations have reported that enhanced EO coefficients are accessible in the presence of a large built-in field induced by the interfaces of GaN/$Al_xGa_{1-x}N$ superlattices. With an Al content of 0.3, the electro-optic coefficients are measured to be 10 times larger than those of GaN bulk material.[13] It is claimed in published literatures that Al composition provides a degree of freedom to control the electro-optic interaction.[14,15] By increasing the barrier content, GaN/$Al_xGa_{1-x}N$ superlattices have much room for promoting the built-in field to enhance optical nonlinearities.

Most experimental studies have been limited to the transparency region of AlGaN. Notably, in the early studies of GaAs, nonlinear absorption occurs near the band edge.[16,17] The resonance effect occurs when photoinduced carriers empty the valence band and fill the conduction band. The resulting transition blocking leads to a nonlinear optical change in the absorption and the refractive index, which rely heavily on the carrier densities near the band edge. Spontaneous polarization and strain-induced polarization lead to a high polarization in AlGaN, resulting in a two-dimensional electron gas at the

Received: April 25, 2015
Accepted: July 23, 2015
Published: August 5, 2015

DOI: 10.1021/acsami.5b06174
ACS Appl. Mater. Interfaces 2015, 7, 17707−17712

interfaces, which has high carrier mobility and electron density in the AlGaN system.[18−20] The existence of resonant optical nonlinearities by modulated field has yet to be explored.

The main interest of this work is to improve the polarity in materials by designing and growing GaN/$Al_xGa_{1-x}N$ quantum structures with an Al content of x = 0.45 using multiple field modulations. A structure with a pair of thin undoped $Al_{0.55}Ga_{0.45}N$ serving as optical confinement layers was proposed to apply an external field effectively on both sides of the quantum structures. The carrier resonance effect was introduced to enhance EO coefficients. The corresponding changes in EO coefficients were derived from the anisotropic refractive indices by fitting the ellipsometric spectra.

EXPERIMENTAL SECTION

The samples were grown on (0001) sapphire substrates by a metal organic vapor phase epitaxy (MOVPE) system (Thomas Swan CCS 3 × 2″). Trimethylgallium, trimethylaluminum, and ammonia were used as the precursors, and high-purity H_2 was used as the carrier gas. SiH_4 was used as the n-type doping source. To verify the results obtained by ellipsometry, a reference sample (marked A) consisting of 2 μm n-type GaN and 15-period GaN/$Al_xGa_{1-x}N$ (x = 0.25) quantumn wells (QWs) was grown. The wells and barriers are 4 and 8 nm thick, respectively. It is recognized that the refraction index of GaN is higher than AlGaN so that the light inside the GaN/$Al_xGa_{1-x}N$ QWs can easily pass through. To enhance the EO effect, we adopted a pair of optical confinement (OC) layers on both sides of the QWs Figure 1a,

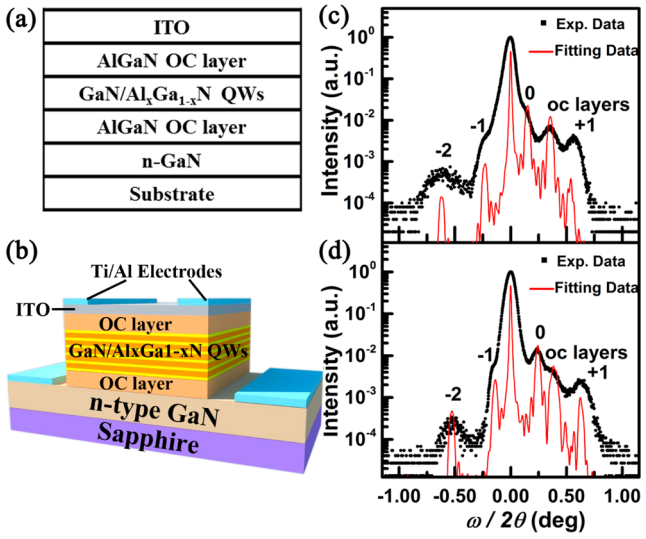

Figure 1. (a) Schematic of the GaN/$Al_xGa_{1-x}N$ QW epitaxy. (b) Schematic of the samples for measuring the EO coefficients with mesa etching and electrodes. XRD scan together with simulation curves of samples (c) B and (d) C.

composed of ∼75 nm thick AlGaN with Al content about 0.55. With the optically thinner $Al_{0.55}Ga_{0.45}N$, the response for the EO effect is improved by extending the optical path length through multiple reflections between the interfaces of QWs and OC layer. The additional high resistivity of the OC layer conducts little current flow beneficial for applying electric fields. For comparison, two samples with the OC layer, denoted as samples B and C, were grown with the Al contents of barrier of 0.25 and 0.45, respectively.

The grown structures were characterized by X-ray diffraction (XRD, X'pert). On the top of the grown wafer, an ITO cladding was deposited by an electron beam evaporation system (VPT Citation). Mesas were etched by a reactive inductively coupled plasma etching system (Oxford Instrument ICP-180), and Ti/Al electrodes were fabricated by electron beam evaporation. The schematic of samples B and C is shown in Figure 1b.

To avoid the thermal effect on the measurement of EO coefficients, pulse DC voltage was applied on the electrodes of the samples from 0 to 20 V at intervals of 2 V. The corresponding variations in anisotropic refractive indices were measured at 300 to 800 nm by spectroscopic ellipsometry (SE). Considering the hexagonal lattice structure of both the GaN and $Al_xGa_{1-x}N$ layers, an uniaxial anisotropy model was built to fit the spectra using Tanguy's dispersion for deriving the anisotropic EO-coefficients.[21,22] To confirm the validity of the above characterization technique, the EO coefficients in sample A without the pair of optical confinement layers were deduced and compared with those in the previous report.[13] The r_{13} and r_{33} in sample A are 4.77 and 16.68 pm/V, respectively, which are consistent with the values of 5.60 and 19.24 pm/V in the superlattice structure with close Al content (approximately 0.3). The present result suggests that ellipsometry is feasible for the detection of EO coefficients.

RESULTS AND DISCUSSION

Grown structures in wafers B and C were first examined by X-ray diffraction (XRD) in $\omega/2\theta$ mode. Satellite peaks up to the second order were identified in Figure 1c, d, indicating the formation of sharp interface and period structures.[23] The strongest peaks found in each XRD curves are from GaN (0002) layers, whereas zeroth-order satellite peaks appear in the right side. The spaces between them increase with the Al content in the quantum wells (QWs). In addition, several satellite peaks array at both sides in the proper order, whereas an obvious peak appears between the zeroth-order and +1-order satellite. This peak comes from the optical confinement (OC) layers with higher Al content. By fitting the experimental curves, the thicknesses of the well and barrier for both wafers are 4 and 8 nm, respectively, whereas the Al contents of the barriers in wafers B and C are 0.25 and 0.45, respectively. Furthermore, the Al contents in the OC layers of these two wafers are both 0.55. These results prove that the grown wafers are fine controlled and agree well with our design.

A follow up SE measurement under different biases were employed in an effort to investigate the optical properties of the grown structures. In the measurements, the ellipsometric parameters Ψ and Δ were obtained directly by SE, where Ψ is the angle whose tangent is the ratio of the p- and s-polarization reflectivity amplitudes and Δ*is* the phase shift in reflection. By ignoring the imperceptible changes in the thicknesses under the external field, the bias-induced variations were examined from the differences between Ψ and Δ*w*ith and without the field, i.e., $\delta\Psi = \Psi(\varsigma) - \Psi(0)$ and $\delta\Delta = \Delta(V) - \Delta(0)$. Figure 2 shows the variations in Ψ and Δ at the visible wavelength range of 500−600 nm for three samples under different fields. As shown in Figure 2a, the variation amplitudes of both Ψ and Δ are distinctly larger in sample B than in sample A. Given that only a pair of OC layers is introduced on both sides of the QWs, the differences are caused by the different structures. Particularly, the electric field in sample B QWs is weaker than that in sample A QWs because the OC layers reduce the electric field. Nonetheless, sample B exhibits a more obvious EO effect at the weaker electric field. When different biases were applied on each sample, the EO effect can change the optical properties differently. The Ψ and Δ variations measured under 4, 8, and −4 V are shown in Figure 2b. For the positive bias, the higher bias can result in larger Ψ and Δ variations. For the negative bias, only slight variations are obtained. This distinct difference can be attributed to the interaction between the external and built-in polarization field.

DOI: 10.1021/acsami.5b06174
ACS Appl. Mater. Interfaces 2015, 7, 17707−17712

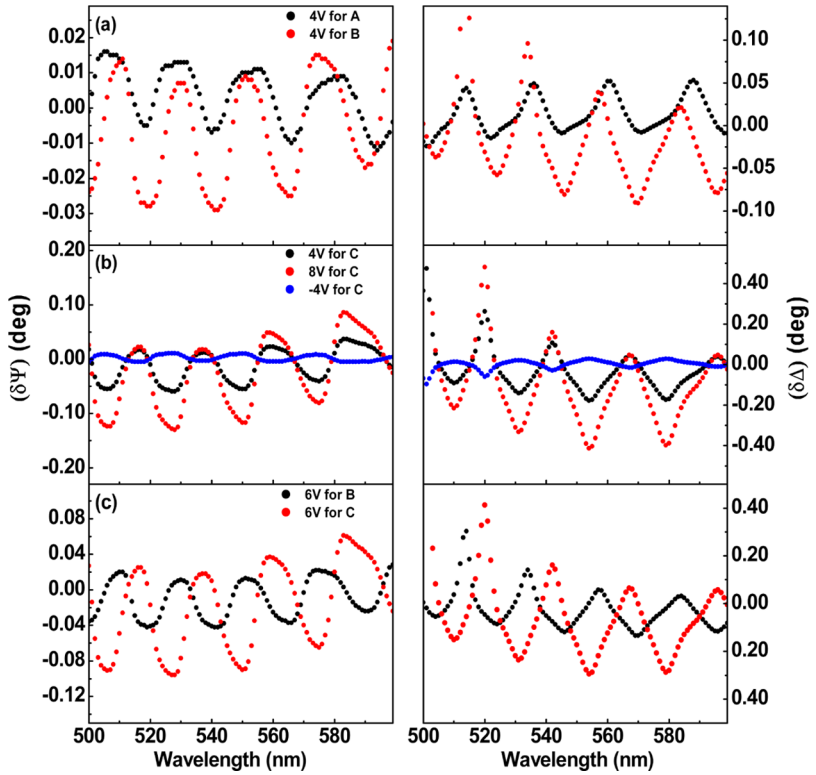

Figure 2. Variations in Ψ and Δ [$\delta\Psi = \Psi(\varsigma) - \Psi(0)$, $\delta\Delta = \Delta(V) - \Delta(0)$] measured in samples A, B, and C at different applied biases. (a) 4 V for samples A and B. (b) −4, 4, and 8 V for sample C. (c) 6 V for samples B and C.

When the electric field and built-in polarization field are in the same direction, they will enhance the EO effect. It is disadvantage for the EO effect when the external and built-in polarization field are in the opposite direction bringing in counteraction between them. Accordingly, the positive bias configuration was applied in our study. As shown in Figure 2c, the amplitude of sample C is larger than that of sample B at the same bias. This finding may be attributed to the higher Al content in the QWs. On the basis of the ellipsometric spectra, the EO effects are believed to be primarily derived from the structure of the designed QWs. In addition, higher Al contents in the QWs result in larger EO effects. Therefore, the EO effects can be controlled and enhanced as our expected design.

It is well-known that the wurtzite crystal structures exist a polarization field in the *c* axis, associated with electrostatic charge densities. This field will influence carrier distributions and consequently electro-optic effects of nitride materials and devices. To understand the polarization field effect, simulations of the band diagram and charge distribution were performed using the Vienna Abinitio Simulation Package (VASP) on GaN/$Al_xGa_{1-x}N$ supercells composed of alternating GaN and AlGaN units. Along *c* axis, the macroscopic electrostatic charge densities were obtained in the Berry phase approach and are estimated to be 2.56×10^{-6} and 5.65×10^{-6} C/cm^2 for GaN/AlN and GaN/$Al_{0.5}Ga_{0.5}N$ higher than bulk GaN,[24] respectively. These results confirmed the increased barrier Al content brings about the increased field, which is expected to enhance optical nonlinearities appearing in the variation of electro-optic coefficients.

To obtain the electro-optic coefficients from the ellipsometric spectra, we fitted the refractive indices under different voltages by a three-phase model. The model includes a substrate, a thin film, and the atmosphere, where the thin film layer is composed of an n-type GaN layer, a pair of $Al_xGa_{1-x}N$ confinement layers, an $Al_xGa_{1-x}N$/GaN QW layer, and an indium tin oxide (ITO) layer. Although the sample contains multiple layers of different structures, its anisotropy can be described by a layered model with *c*-axis orientation according to the XRD results. Figure 3a, b shows the typical ordinary and extradinary refractive index of sample C with voltages of 0 and 20 V, repectively. In our previous study on AlN, the ellipsometric spectra were represented well by

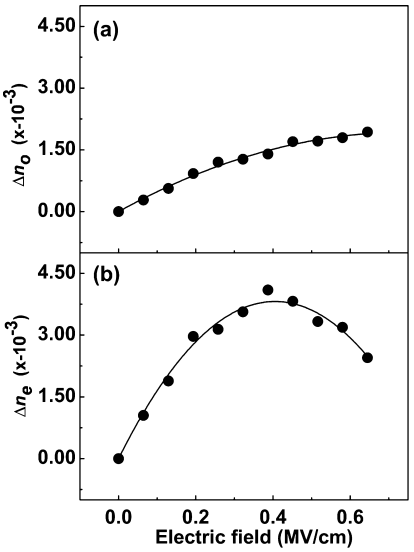

Figure 3. Variation in (a) extraordinary indices and (b) ordinary indices in sample C as a function of different applied biases by fitting eq 2.

DOI: 10.1021/acsami.5b06174
ACS Appl. Mater. Interfaces 2015, 7, 17707−17712

Tanguy's dispersion formula.[25] However, they are very sensitive to optical anisotropy.

With the fitting results from 300 to 800 nm, the optical parameters under different biases and the thickness were obtained. The thicknesses of the QW layers (d_{QWs}) of samples B and C are 174 and 179 nm, respectively, which are consistent with the XRD measurements. This finding indicates the reliability of the SE results. Thus, the obtained thickness, including that of the OC layers (d_{oc}), can be used to evaluate the electric field. Given that the conductivities of n-type AlGaN or ITO are much higher than that of QWs, a large part of the voltage was loaded on both sides of the QWs. The electric field in the QWs can be approximately described as

$$E_{QWs} = \frac{V_{QWs}}{d_{QWs}} \quad (1)$$

With regard to the high resistance of AlN,[26] the AlGaN resistivity in the OC layer and QWs is at least 1×10^{12} orders of magnitude larger than that of *n*-type GaN[27] and ITO.[28] The highly resistive OC layers and QWs connecting in series conduct little current flow while applying limited voltage. On account of the same magnitude of the resistivity between OC layers and QWs, it is sensible to simplify these two layers approximately having the same resistivity in order to capture the essential physics for understanding the EO effect. Here, $V_{QWs} = (d_{QWs}/(2d_{oc} + d_{QWs}))V$. Thus, the electric field intensity is up to 0.6 MV/cm in the QWs when a 20 V bias is applied to samples B and C. Figure 3c, d exhibits the bias dependent variations of ordinary and extraordinary refractive indices, $\Delta n_o = n_o(V) - n_o(0)$ and $\Delta n_e = n_e(V) - n_e(0)$, in sample C at a visible wavelength of 632 nm. With increasing electric field, both Δn_o and Δn_e monotonously increase in the weaker field region. As the electric field reaches a certain high level, the nonlinear modulation of refractive indices can be distinctly recognized. Particularly, for Δn_e, the curve shows a downward trend with increasing electric field.

It is noted that the interface between GaN and AlGaN heterojunction is subject to a large lattice mismatch, which produces the built-in field via the corresponding polarization effect. When a sufficiently large external electric field is applied, the EO effect will impact the light propagation under the superposition of the built-in and external electric fields, thereby rendering a change in refractive index as a macro representative. We found that EO can be tuned by modulating the external electric field. Moreover, when the electric field reaches a sufficiently large level, not only the linear EO effects but also the higher-order, especially second-order, EO effects will be on the incident light (Figure 3).

Given the hexagonal symmetry of III-nitride QWs, two nonzero EO coefficient tensors, r_{13} and r_{33}, correspond to Δn_o and Δn_e. These variations under the external electric field are written as

$$\Delta n_o = -\frac{1}{2} n_o^3 (r_{13} E_z + R_{13} E_z^2)$$

$$\Delta n_e = -\frac{1}{2} n_e^3 (r_{33} E_z + R_{33} E_z^2) \quad (2)$$

By employing these formulas to fit the results in Figure 3, the EO coefficients were obtained. For sample C, the EO coefficients at 632 nm are $r_{13} = 8.4$, $R_{13} = -5.5$, $r_{33} = 30.5$, and $R_{33} = -37.9$. The EO coefficients of extraordinary indices (r_{33} and R_{33}) are larger than those of ordinary indices (r_{13} and R_{13}). By increasing Al content, the enhancement of EO coefficients taking steps ahead of values reported in the literature.[13] This result may be attributed to the maximum coupling between the vertical external electric field and the extraordinary light whose electric vector is parallel to the external electric field.

Arisen from absorption-induced photocarriers, resonant nonlinearities building up a field modulation would provide enhanced performance in GaN/AlGaN superlatices. To investigate this influence to the EO effect, we extended the dispersion measurement of EO coefficients in sample C to the band edge. Different from the transparent range characterized by approximately constant values, the EO coefficient dispersions at 300 to 450 nm dramatically increase and reach their maximum in the UV region at 360 nm (Figure 4).

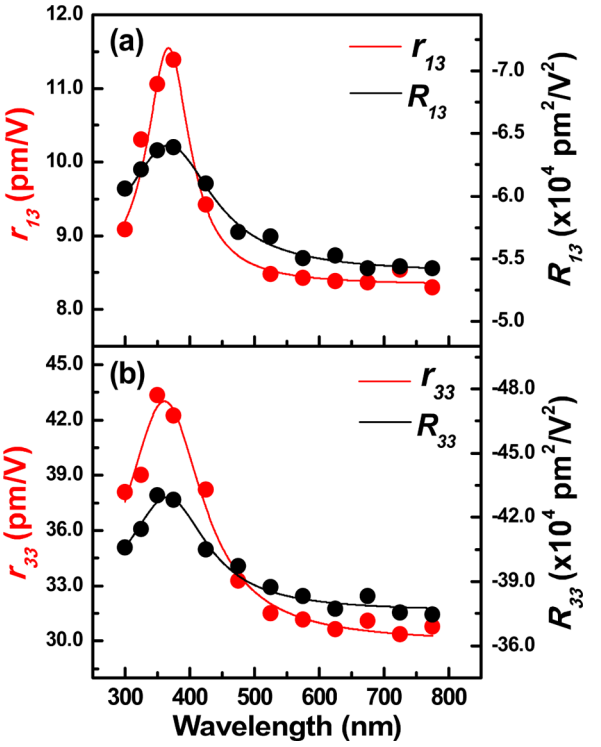

Figure 4. Dispersions of EO coefficients for sample C at 300 to 800 nm. (a) Linear EO coefficients. (b) Quadratic EO coefficients.

Particularly, the Pockels coefficients (r_{13} and r_{33}) near the band gap increase by almost 50% compared with those in the visible region. As semiconductor materials, the resonance of photo-induced carriers in QWs is responsible for the enhancement of the EO coefficients near the band edge.[29] Particularly, the excitons in QWs have a large dipole moment and thus can significantly enhance the second-order nonlinear optic effects. This finding accounts for the more obvious enhancement of Pockels coefficients than Kerr coefficients (R_{13} and R_{33}).

When the wavelength reaches the resonance energy at the band edge or higher, the thin well layers are less absorptive than thick layers of the same composition and allow relatively more high frequency photons to come through. Photoinduced carriers fill available states with increased sensitivity of the state-filing optical nonlinearity.[31] To determine a figure of merit, the derived EO coefficients of our samples at 632 nm, as well as bulk $Al_{0.45}Ga_{0.55}N$, KDP and LN, are listed in Table 1. The EO coefficients of samples B and C are comparable with

DOI: 10.1021/acsami.5b06174
ACS Appl. Mater. Interfaces 2015, 7, 17707−17712

Table 1. Linear and Quadratic EO Coefficients of Samples B and C in Comparison with Those of Bulk $Al_{0.45}Ga_{0.55}N$, KDP, and LN[30]

	sample B GaN/$Al_{0.25}Ga_{0.75}N$	sample C GaN/$Al_{0.45}Ga_{0.55}N$		bulk $Al_{0.45}Ga_{0.55}N$	KDP (KH_2PO_4)	LN ($LiNbO_3$)
	632 nm	632 nm	∼ 360 nm	633 nm	546.1 nm	500 nm
linear EO coefficients r_{ij} (pm/V)	r_{13} = 6.24 ± 0.3	r_{13} = 8.4 ± 0.3	r_{13} = 11.4 ± 0.4	r_{13} = 0.49	r_{41} = 8.8	r_{13} = 9.6 r_{22} = 6.8 r_{33} = 30.9
quadratic EO coefficients R_{ij} ($\times 10^4$ pm^2/V^2)	r_{33} = 20.1 ± 0.7 R_{13} = −3.8 ± 0.2 R_{33} = −25.1 ± 1.3	r_{33} = 30.5 ± 0.8 R_{13} = −5.5 ± 0.3 R_{33} = −37.9 ± 1.6	r_{33} = 43.3 ± 1.0 R_{13} = −6.4 ± 0.4 R_{33} = −42.9 ± 1.8	r_{33} = 0.78	r_{63} = 10.5	r_{42} = 32.6

that of $Al_{0.45}Ga_{0.55}N$, which interpolated from literature values for GaN[32] and AlN.[33] Especially, the larger EO coefficients of sample C at 360 nm with higher Al contents (x = 0.45) subject to large built-in and external fields in $Al_xGa_{1-x}N$/GaN QWs are attributed to the resonance effect. Moreover, the EO coefficients of our designed structural materials are currently competitive with those of traditional electro-optic crystals, such as KDP and LN. More importantly, the EO coefficients of our designed structural materials were underestimated in our calculations because we assumed that the whole voltage was loaded on this active region, given that the resistivity of the active region was much larger than that of the n-type GaN and the top ITO. In fact, a certain voltage is still applied on the n-type GaN layer and ITO layer. This finding indicates that the EO effect is generated at the lower electric field intensity and that the EO coefficients of the designed structures should be larger than the obtained values. Accordingly, our designed structures have the advantage of the EO coefficients. With their higher optical response, they are easier to integrate in GaN-based devices, such as all-optic switch, EO phase modulator, and so on, compared with traditional EO materials. Therefore, the designed structures may have significant applications in information optoelectronics in the future.

CONCLUSIONS

In summary, $Al_xGa_{1-x}N$/GaN QWs with an enhanced EO effect were designed by multiple field modulations. Increasing Al contents up to x = 0.45 allows for an enhanced nonlinear response in $Al_xGa_{1-x}N$/GaN QWs. This response shows a growing tendency with increasing Al content. Sandwiched between a pair of undoped optical confinement layers, the $Al_xGa_{1-x}N$/GaN QWs exhibit significant changes in their ellipsometric spectra under a high intensity of external field. By fitting the variable-angle SE, the dispersions of two linear EO coefficients, r_{13} and r_{33}, were determined from extraordinary and ordinary refractive indices. Moreover, the relatively quadratic EO coefficients were deduced with the high electric field. Combined with resonance effect, our designed structures provide enhanced EO effect in the UV region near the band edge. Our structures can challenge state-of-the-art nonlinear crystals. This improvement renders AlGaN as a unique and promising family of nonlinear optical materials that can be used for the integration of many functions with mature GaN-based UV devices in optical information technology.

AUTHOR INFORMATION

Corresponding Authors

*E-mail: linwei@xmu.edu.cn. Phone: +86-592-2187537. Fax: +86-592-2187737.

*E-mail: jykang@xmu.edu.cn. Phone: +86-592-2185962. Fax: +86-592-2187737.

Author Contributions

W.J. assembled the data, conceived the study, and wrote the first draft of the manuscript with W.Y.P.; all authors participated in writing the manuscript and discussion of the results; W.L. and J.Y.K. contributed to the revision of the final manuscript. All authors have given approval to the final version of the manuscript.

Notes

The authors declare no competing financial interest.

ACKNOWLEDGMENTS

This work was supported by Chinese National Key Project "973" (2012CB619301 and 2011CB925600), the "863" program (2014AA032608), the National Nature Science Foundation of China (U1405253, 11404271, 11304257, 61227009, and 11204254), the Fundamental Research Funds for the Central Universities (20720150027), and the Natural Science Foundations of Fujian Province (2014J01026 and 2015J01028).

REFERENCES

(1) Lu, H.; Sadani, B.; Ulliac, G.; Courjal, N.; Guyot, C.; Merolla, J.-M.; Collet, M.; Baida, F. I.; Bernal, M.-P. 6-Micron Interaction Length Electro-Optic Modulation Based On Lithium Niobate Photonic Crystal Cavity. *Opt. Express* **2012**, *20*, 20884−20893.

(2) Huo, J.; Liu, K.; Chen, X. 1 × 2 Precise Electro-Optic Switch In Periodically Poled Lithium Niobate. *Opt. Express* **2010**, *18*, 15603−15608.

(3) Lin, S.-T.; Hsieh, C.-S. Triple-Wavelength Nd-Laser System By Cascaded Electro-Optic Periodically Poled Lithium Niobate Bragg Modulator. *Opt. Express* **2012**, *20*, 29659−29664.

(4) Zhou, X.; Wenqiong, G.; Xiongjun, Z.; Zhan, S.; Dengsheng, W. One-Dimensional Model Of A Plasma-Electrode Optical Switch Driven By One-Pulse Process. *Opt. Express* **2006**, *14*, 2880−2887.

(5) Wu, H.; Yu, H.; Pan, S.; Huang, Z.; Yang, Z.; Su, X.; Poeppelmeier, K. R. Cs2B4SiO9: A Deep-Ultraviolet Nonlinear Optical Crystal. *Angew. Chem., Int. Ed.* **2013**, *52*, 3406−3410.

(6) Pu, Y.; Grange, R.; Hsieh, C.-L.; Psaltis, D. Nonlinear Optical Properties Of Core-Shell Nanocavities For Enhanced Second-Harmonic Generation. *Phys. Rev. Lett.* **2010**, *104*, 207402.

(7) Han, J.; Crawford, M. H.; Shul, R. J.; Figiel, J. J.; Banas, M.; Zhang, L.; Song, Y. K.; Zhou, H.; Nurmikko, A. V. Algan/Gan Quantum Well Ultraviolet Light Emitting Diodes. *Appl. Phys. Lett.* **1998**, *73*, 1688.

(8) Nakamura, S.; Senoh, M.; Mukai, T. High-Power Ingan/Gan Double-Heterostructure Violet Light Emitting Diodes. *Appl. Phys. Lett.* **1993**, *62*, 2390.

(9) Rigutti, L.; Tchernycheva, M.; De Luna Bugallo, A.; Jacopin, G.; Julien, F. H.; Zagonel, L. F.; March, K.; Stephan, O.; Kociak, M.; Songmuang, R. Ultraviolet Photodetector Based On Gan/Aln

DOI: 10.1021/acsami.5b06174
ACS Appl. Mater. Interfaces 2015, 7, 17707−17712

Quantum Disks In A Single Nanowire. *Nano Lett.* **2010**, *10*, 2939−2943.
(10) Leuthold, J.; Koos, C.; Freude, W. Nonlinear Silicon Photonics. *Nat. Photonics* **2010**, *4*, 535−544.
(11) Miragliotta, J.; Wickenden, D. K.; Kistenmacher, T. J.; Bryden, W. A. Linear- And Nonlinear-Optical Properties Of Gan Thin Films. *J. Opt. Soc. Am. B* **1993**, *10*, 1447.
(12) Miragliotta, J.; Wickenden, D. Nonlinear Electroreflectance From Gallium Nitride Using Optical Second-Harmonic Generation. *Phys. Rev. B: Condens. Matter Mater. Phys.* **1996**, *53*, 1388−1397.
(13) Chen, P.; Tu, X. G.; Li, S. P.; Li, J. C.; Lin, W.; Chen, H. Y.; Liu, D. Y.; Kang, J. Y.; Zuo, Y. H.; Zhao, L.; Chen, S. W.; Yu, Y. D.; Yu, J. Z.; Wang, Q. M. Enhanced Pockels Effect In Gan/$A_{1-X}ga_xn$ Superlattice Measured By Polarization-Maintaining Fiber Mach-Zehnder Interferometer. *Appl. Phys. Lett.* **2007**, *91*, 031103.
(14) Driscoll, K.; Bhattacharyya, A.; Moustakas, T. D.; Paiella, R.; Zhou, L.; Smith, D. J. Intersubband Absorption In Aln/Gan/Algan Coupled Quantum Wells. *Appl. Phys. Lett.* **2007**, *91*, 2007−2009.
(15) Xiong, C.; Pernice, W. H. P.; Tang, H. X. Low-Loss, Silicon Integrated, Aluminum Nitride Photonic Circuits And Their Use For Electro-Optic Signal Processing. *Nano Lett.* **2012**, *12*, 3562−3568.
(16) Said, A. A.; Sheik-Bahae, M.; Hagan, D. J.; Wei, T. H.; Wang, J.; Young, J.; Van Stryland, E. W. Determination Of Bound-Electronic And Free-Carrier Nonlinearities In Znse, Gaas, Cdte, And Znte. *J. Opt. Soc. Am. B* **1992**, *9*, 405.
(17) Malevich, V. L.; Utkin, I. A. Nonlinear Optical Absorption In A Heavily Doped Degenerate N-Gaas. *Semiconductors* **2000**, *34*, 924−926.
(18) Ibbetson, J. P.; Fini, P. T.; Ness, K. D.; DenBaars, S. P.; Speck, J. S.; Mishra, U. K. Polarization Effects, Surface States, And The Source Of Electrons In Algan/Gan Heterostructure Field Effect Transistors. *Appl. Phys. Lett.* **2000**, *77*, 250.
(19) Keller, B. P.; Keller, S.; Kapolnek, D.; Jiang, W. N.; Wu, Y. F.; Masui, H.; Wu, X.; Heying, B.; Speck, J. S.; Mishra, U. K.; Denbaars, S. P. Metalorganic Chemical Vapor Deposition Growth Of High Optical Quality And High Mobility Gan. *J. Electron. Mater.* **1995**, *24*, 1707−1709.
(20) Smorchkova, I. P.; Elsass, C. R.; Ibbetson, J. P.; Vetury, R.; Heying, B.; Fini, P.; Haus, E.; DenBaars, S. P.; Speck, J. S.; Mishra, U. K. Polarization-Induced Charge And Electron Mobility In Algan/Gan Heterostructures Grown By Plasma-Assisted Molecular-Beam Epitaxy. *J. Appl. Phys.* **1999**, *86*, 4520.
(21) Tanguy, C.; Lefebvre, P.; Mathieu, H.; Elliott, R. J. Analytical Model For The Refractive Index In Quantum Wells Derived From The Complex Dielectric Constant Of Wannier Excitons In Noninteger Dimensions. *J. Appl. Phys.* **1997**, *82*, 798.
(22) Tanguy, C. Optical Dispersion By Wannier Excitons. *Phys. Rev. Lett.* **1995**, *75*, 4090−4093.
(23) Asif Khan, M.; Kuznia, J. N.; Olson, D. T.; George, T.; Pike, W. T. Gan/Aln Digital Alloy Short-Period Superlattices By Switched Atomic Layer Metalorganic Chemical Vapor Deposition. *Appl. Phys. Lett.* **1993**, *63*, 3470−3472.
(24) Nardelli, M. B.; Rapcewicz, K.; Bernholc, J. Strain Effects On The Interface Properties Of Nitride Semiconductors. *Phys. Rev. B: Condens. Matter Mater. Phys.* **1997**, *55*, R7323−R7326.
(25) Jiang, W.; Lin, W.; Li, S.; Chen, J.; Kang, J. Optical Anisotropy Of Aln Epilayer On Sapphire Substrate Investigated By Variable-Angle Spectroscopic Ellipsometry. *Opt. Mater. (Amsterdam, Neth.)* **2010**, *32*, 891−895.
(26) Claudel, a.; Blanquet, E.; Chaussende, D.; Boichot, R.; Doisneau, B.; Berthomé, G.; Crisci, A.; Mank, H.; Moisson, C.; Pique, D.; Pons, M. Epitaxial And Polycrystalline Growth Of Aln By High Temperature CVD: Experimental Results And Simulation. *J. Cryst. Growth* **2011**, *335*, 17−24.
(27) Yamamoto, A.; Yamaguchi, S. Thermoelectric Properties Of Hot-Pressed Gan And Inn. *MRS Online Proc. Libr.* **2003**, *793*, S8.24.
(28) Ellmer, K. Past Achievements And Future Challenges In The Development Of Optically Transparent Electrodes. *Nat. Photonics* **2012**, *6*, 809−817.
(29) Kawase, M.; Garmire, E.; Lee, H. C.; Dapkus, P. D. Single-Pulse Pump-Probe Measurement Of Optical Nonlinear Properties In Gaas/Algaas Multiple Quantum Wells. *IEEE J. Quantum Electron.* **1994**, *30*, 981−988.
(30) Boyd, R. W. *The Electrooptic And Photorefractive Effects*, 3rd ed.; World Publishing Corporation: Beijing, 2008.
(31) Döhler, G. H. Semiconductor Superlattices-A New Material For Research And Applications. *Phys. Scr.* **1981**, *24*, 430−439.
(32) Long, X.-C.; Myers, R. a.; Brueck, S. R. J.; Ramer, R.; Zheng, K.; Hersee, S. D. GaN Linear Electro-Optic Effect. *Appl. Phys. Lett.* **1995**, *67*, 1349−1351.
(33) Gräupner, P.; Pommier, J. C.; Cachard, a.; Coutaz, J. L. Electro-Optical Effect In Aluminum Nitride Waveguides. *J. Appl. Phys.* **1992**, *71*, 4136−4139.

DOI: 10.1021/acsami.5b06174
ACS Appl. Mater. Interfaces 2015, 7, 17707−17712